THE JOURNAL OF PHYSICAL CHEMISTRY B

Article

pubs.acs.org/JPCB

Microheterogeneity in Native and Cation-Exchanged Nafion Membranes

E. Siva Subramaniam Iyer and Anindya Datta*

Department of Chemistry, Indian Institute of Technology Bombay, Mumbai, India 400076

ABSTRACT: 2-(4′-Pyridyl)benzimidazole (4PBI) has been used to investigate the microheterogeneity of water nanochannels of Nafion membranes at two different hydration levels. Native as well as cation-exchanged Nafion membranes are found to protonate one of the two monoprotonated forms of 4PBI selectively. In native membranes and in those in which H_3O^+ ions are replaced by $(CH_3)_4N^+$ ions, the pyridyl nitrogen is protonated preferentially. In Na^+-exchanged membranes, however, the benzimidazole nitrogen is protonated selectively. Unlike other fluorescent probes used in earlier studies, 4PBI can differentiate between the two different cation-exchanged membranes at lower as well as higher hydration levels.

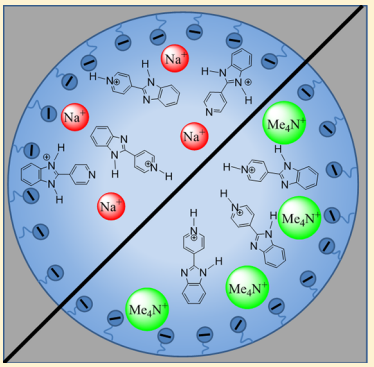

INTRODUCTION

Nafion membranes find application in fuel cells,[1] catalysis,[2] and ion-exchange resins.[3] Their chemical structure comprises a hydrophobic Teflon backbone and hydrophilic, negatively charged pendant sulfonate groups (Scheme 1).[4,5] They can take up significant amounts of water to form a network of water channels. Nafion exhibits marked permselectivity and high proton conductivity. Factors such as the water content, temperature, and counterions present in the membranes affect the proton conductivity significantly.[6−8] The properties of Nafion are generally described in light of the cluster network model in which the water channels collapse to form isolated water clusters upon decreasing the water content, thereby causing a decrease in the proton conductivity.[9,10] Even though the cluster network model is widely accepted, there are other schools of thought as well. An example is the parallel network model according to which the channels have diameters of about 2.4 nm with hydrophilic groups aligned inside resembling cylindrical reverse micelles.[7] These relatively wide channels favor a large hydrodynamic component of water transport. A new topology, resulting from the random connectivity of water channels, is obtained at low water contents. Thus, water transport is enabled under these conditions. Even though this model is limited to lengths of a few tens of nanometers, its appeal lies in the successful prediction of proton conductivity at lower temperatures, at which the cluster model is unsuccessful. Some other relevant models involve polymer bundles in a hydrated matrix,[11−13] hydrated bilayer stacks,[14] a network model,[15,16] and alternate polymer−water layers.[9]

Scheme 1. Chemical Structure of Nafion

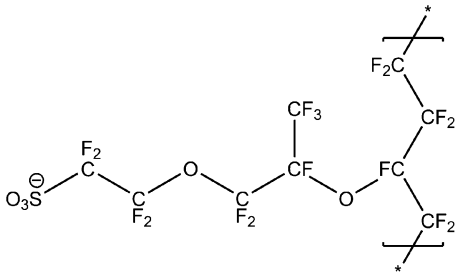

In recent times, we have investigated the dynamics of proton transfer in the Nafion membranes.[17−19] Using fluorescent probes Coumarin 102 (C102)[20] and 2-(2′-pyridyl)-benzimidazole (2PBI),[21] we have observed that electrostatic interactions between the mobile cations and the negatively charged sulfonate groups have a rather significant effect on the mobility of cations in Nafion at low water contents. This is manifested in the slowing down of excited-state proton transfer (ESPT) on molecular length scales. Moreover, at lower water content, Nafion is found to stabilize unusual ground and excited states of (2,2′-bipyridyl)-3,3′-diol ($BP(OH)_2$).[17] This phenomenon bolstered the contention of decreased proton mobility at lower water contents because of a greater extent of electrostatic interactions. The exchange of mobile H_3O^+ ions with cations such as Na^+ or $(CH_3)_4N^+$ causes a decrease in the acidity as well as the water content in the water channels. However, the fluorescent probes used so far have been unable to differentiate between the environments of partially dried Na^+-exchanged and $(CH_3)_4N^+$-exchanged membranes because they undergo proton transfer only in their protonated forms and the extent of protonation is the same in membranes containing different cations. Upon displacement of H_3O^+ ions with Na^+ or

Received: April 24, 2012
Revised: July 28, 2012
Published: July 31, 2012

Scheme 2. Protonation−Deprotonation Equilibria Operative in 4PBI[a]

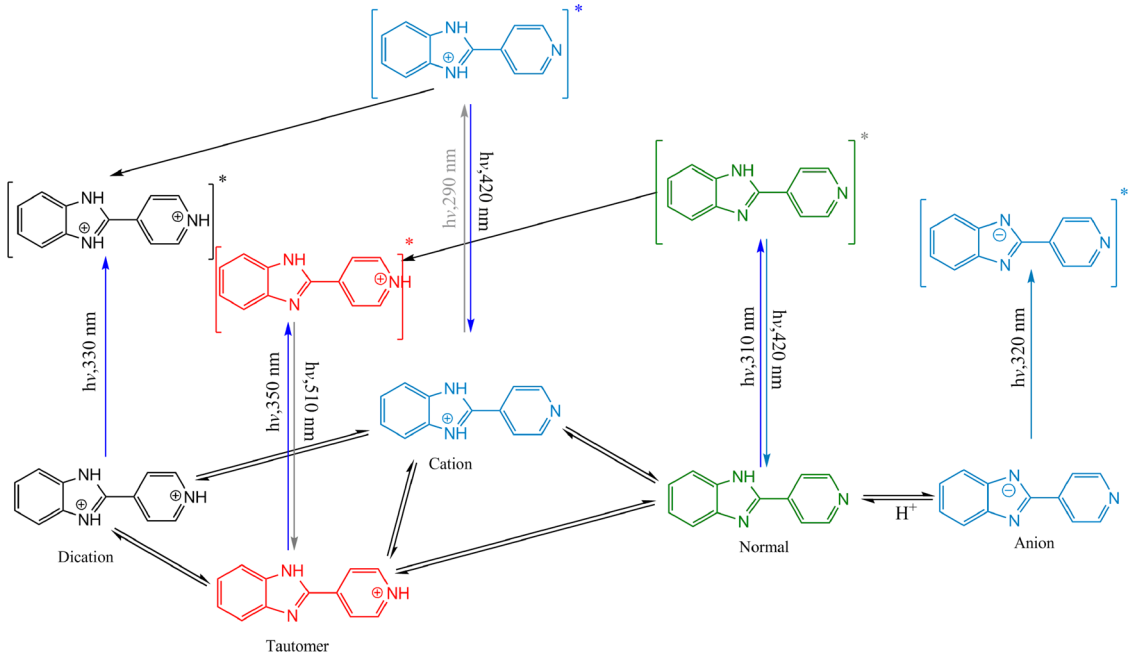

[a]This scheme has been reproduced from ref 22 with some changes.

$(CH_3)_4N^+$ ions, C102 exists in its neutral form rather than in the protonated form.[20] For 2PBI, the dicationic form that is present in the native membranes makes way for the monoprotonated cation.[21] This is the major motivation for the present study with 2-(4′-pyridyl)benzimidazole (Scheme 2), a positional isomer of 2PBI, in Nafion. Unlike 2PBI, the tautomer form of this molecule, in which the pyridyl nitrogen is protonated, coexists in the ground state along with the cation form, in which the second benzimidazole nitrogen atom is protonated in aqueous solutions of pH 3−8.[22−24] The existence of an additional tautomer in the ground state in a moderate pH range makes this fluorophore a better candidate for sensing the difference in the microenvironments of differently cation-substituted Nafion. Besides, the interpretation of the fluorescence experiments, performed in complex microenvironments such as that of the water channels of Nafion, needs to be done very carefully because there are many factors that might affect the fluorescence of a particular fluorophore. To develop a complete picture of the system, it is essential to perform the studies with related but different fluorophores.

EXPERIMENTAL SECTION

Nafion 117 membranes and 2-(4′-pyridyl)benzimidazole (4PBI) are from Aldrich. 4PBI is recrystallized from a mixture of ethanol and water prior to use. The membranes are cleaned by heating with 5% H_2O_2 solution for 3 h, followed by heating in water, and 1 M HNO_3. The procedure is repeated until transparent membranes are obtained. The membranes are dipped in aqueous solution of 4PBI (with absorbance ∼1) until the absorbance of membrane is approximately 0.5 at the absorption maximum. Excess dye on the surface is removed by rinsing with water. The membranes with a lower water content are obtained by heating in vacuum to 70 °C until no change in the weight of the membranes is observed. The dried membranes are kept in sealed cuvettes during the course of experiment to avoid the uptake of water by membranes from the atmosphere. The hydrated membrane contains ∼10% w/w water, which is the weight lost upon drying. This corresponds to $\lambda = 6$ in hydrated membranes and $\lambda = 1$ in less-hydrated membranes,[25] where λ is the ratio of the number of equivalents of water to that of sulfonate groups. It may be noted that the complete removal of water from Nafion membranes is never possible. The cation-exchanged membranes have been obtained by keeping the native membranes immersed either in 1 M NaOH or in a 1 M $(CH_3)_4NCl$ solution for 24 h.

The steady-state absorption spectra have been recorded on a Jasco V530 absorption spectrophotometer, and the fluorescence spectrum is recorded with a Varian Cary Eclipse spectrofluorimeter. The time-resolved experiments are performed with an IBH Horiba-JY fluorocube. The sample is excited by NanoLED emitting at 340 nm (fwhm = 750 ps) and NanoLED at 295 nm (fwhm = 700 ps). The membrane is kept at 45° with respect to the excitation source such that the excitation light is directed opposite to the detector, and fluorescence is collected from the back surface of the membrane. The decays are recorded at magic angle polarization with respect to the polarization of the incident light. The data obtained is fitted to multiexponential models by Picoquant Fluofit data analysis software using an iterative reconvolution technique.

RESULTS AND DISCUSSION

The absorption spectrum of 4PBI in native Nafion at $\lambda = 6$ exhibits a maximum at 338 nm with a shoulder at 280 nm. The fluorescence maximum occurs at 480 nm (Figure 1). The excitation and absorption spectra are superimposable with each other. The 280 nm shoulder can be assigned to the cation, C, and the major band at 338 nm can be assigned to the dication, D.[22] The fluorescence spectrum is that of the tautomer, whose excited state is denoted as T*.[22] The position of the fluorescence maximum does not depend on the excitation wavelength, nor does the fluorescence excitation spectrum

dx.doi.org/10.1021/jp303924a | J. Phys. Chem. B 2012, 116, 9992−9998

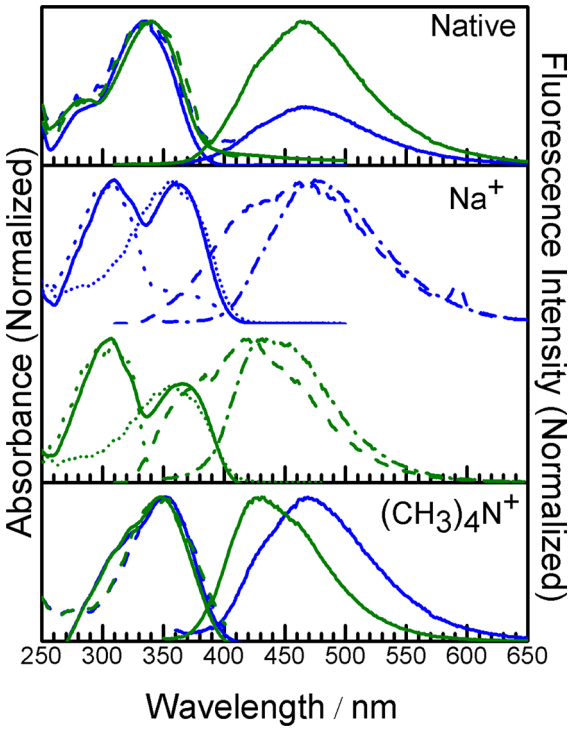

Figure 1. Steady-state spectra of 4PBI in native, Na^+-exchanged, and $(CH_3)_4N^+$-exchanged Nafion membranes at λ = 6 (blue) and 1 (green). Absorption spectra are shown by solid lines. In native and $(CH_3)_4N^+$-exchanged Nafion, the fluorescence spectra (λ_{ex} = 340 nm) are shown by solid lines and the excitation spectra (λ_{em} = 500 nm) are shown by dashed lines. In Na^+-exchanged Nafion, fluorescence spectra with λ_{ex} = 295 and 340 nm are shown by dashed and dashed−dotted lines, respectively, whereas excitation spectra are shown by dots (λ_{em} = 400 nm) and short dots (λ_{em} = 500 nm).

change with the wavelength at which the fluorescence is monitored. It may be inferred that the locally excited state, D*, undergoes excited-state deprotonation from a benzimidazole nitrogen atom in Nafion, presumably because of the very low pK_a* (= 1) of this nitrogen atom.[22] This is reminiscent of our earlier observations with a positional isomer, 2PBI, in the Nafion membrane. 2PBI also exists in a dicationic form in its ground state within the nanochannels of Nafion but undergoes the loss of a proton in the excited state.[19] However, it is also possible that the absorption spectrum of T has a tail at 280 nm and direct T → T* excitation occurs even at this wavelength. There is no change in the shape or spectral maxima of the steady-state spectra upon drying the membrane to λ = 1. However, the relative quantum yield increases by a factor of 2.5 (Figure 1). The invariance of the steady-state spectra upon a change in water content seems to indicate that the fluorophore resides near the interface and hence the environment around the fluorophore is not significantly affected by the water content. The ground and excited states of the fluorophore in the dried membrane are thus found to be the same as the corresponding states in the membrane with λ = 6. This behavior is different from that of the two fluorophores that we studied earlier in Nafion. In C102, the dehydration of the membrane does not affect the ground state of the fluorophore, but excited-state proton transfer is hindered, which is reflected in the fluorescence spectrum. In case of 2PBI, both the absorption and fluorescence spectra are found to be affected upon dehydration, indicating a modification in ground- as well as excited-state processes. The emission spectra of C102 and 2PBI exhibit broadening and a blue shift upon the dehydration of Nafion to λ = 1, indicating that these fluorophores experience a greater microheterogeneity in the environment upon drying.[20,21]

Fluorescence decays of 4PBI in Nafion are biexponential, with components of approximately 2 and 6 ns in hydrated membranes (λ = 6, Figure 2a, Table 1). The decays become

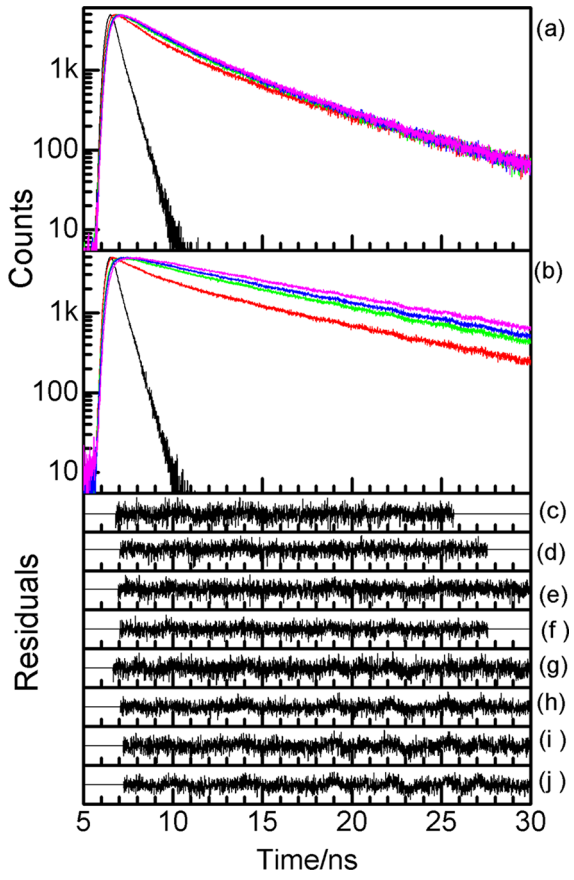

Figure 2. (a, b) Fluorescence decays of 4PBI at λ_{ex} = 340 nm and λ_{em} = 395 nm (red), 440 nm (green), 465 nm (blue), and 520 nm (pink) in Nafion membranes at (a) λ = 6 and (b) λ = 1. (c−j) Weighted residuals for fits to the data in a and b. (c−f) λ = 6: λ_{em} = (c) 395 nm, (d) 440 nm, (e) 465 nm, and (f) 520 nm. (g−j) λ = 1: λ_{em} = (g) 395 nm, (h) 440 nm, (i) 465 nm, (j) 520 nm.

slightly slower at longer emission wavelengths. A markedly stronger wavelength dependence is observed upon dehydration of the membrane to λ = 1 (Figure 2b). At this level of hydration, the 2 ns component persists but the longer component is slowed down to 9 ns in the blue edge of the emission spectrum. The amplitude of the shorter component decreases progressively with increase in the emission wavelengths until the decays become monoexponential at the longest emission wavelengths recorded. There is a concomitant increase in the lifetime to 11 ns. This is interesting, especially because there is no change in the shape of the steady-state fluorescence spectrum upon drying (Figure 1). This difference in the behavior of 4PBI from the other two fluorophores can be rationalized as follows. The ESPT in 2PBI and C102 are affected at lower levels of hydration. However, in 4PBI, the ground state is a mixture of D and T forms. T* fluorescence occurs from excited states formed by the direct excitation of

dx.doi.org/10.1021/jp303924a | J. Phys. Chem. B 2012, 116, 9992−9998

Table 1. Temporal Features of the Fluorescence of 4PBI in Native Nafion at Higher Hydration ($\lambda = 6$) and Lower Hydration ($\lambda = 1$) Levels

	$\lambda = 6$					$\lambda = 1$				
λ_{em}/nm	τ_1/ns	τ_2/ns	a_1	a_2	χ^2	τ_1/ns	τ_2/ns	a_1	a_2	χ^2
395	5.20	1.37	0.36	0.64	1.00	9.07	1.94	0.36	0.64	1.08
440	5.80	2.01	0.36	0.64	1.06	9.67	2.34	0.77	0.23	1.13
465	5.32	1.87	0.46	0.54	1.05	9.76	2.22	0.85	0.15	1.14
520	5.44	1.98	0.44	0.56	1.11	10.57		1.00		1.20

4PBI molecules in the T form as well as, possibly, by D* → T* transitions. If T* is formed from D* by the loss of a proton, then it is the imidazole nitrogen that is lost. The selective loss of a proton from the imidazole nitrogen, rather than from the pyridyl nitrogen, may be rationalized by the fact that the pK_a* of pyridyl nitrogen is 14 and that of imidazole nitrogen is 4.8.[22] Thus the imidazole nitrogen has a greater tendency to lose its proton in the excited state. In such a case, a rise time in the T* emission might have been expected. Its absence denotes that the loss of a proton, if it takes place, is ultrafast and is missed in the present experiments. With D* being nonfluorescent, the two lifetimes of 2 and 6 ns are ascribed to T* in different environments inside the Nafion membrane. The 2 ns component can be assigned to the fluorophores in the more waterlike region whereas the 6 ns component can be assigned to fluorophores in the vicinity of the sulfonate groups. This is a simplified model that describes the distribution of the cationic fluorophore molecules in the microheterogeneous environment of Nafion, arising by virtue of their electrostatic attraction to the sulfonate groups. The distribution of population is expected to show up in the fluorescence quantum yield and lifetimes but not in the spectral shape or position for 4PBI because it does not exhibit a marked dependence of the fluorescence maximum on the properties of its microenvironment. The increase in the fluorescence quantum yield upon dehydration of the membrane may be attributed to a decrease in fluorescence quenching by water, which is manifested in the increase in the longer lifetime. However, this is not the only effect that is operative because the amplitude of the shorter component decreases upon dehydration, indicating that the population of fluorophores in the waterlike environment decreases. This observation is in line with our proposed model of increased electrostatic interaction at lower water content. The increase in the value of the longer lifetime with increases in the fluorescence wavelength indicates a population distribution of fluorophores at different distances from the sulfonate group, even at $\lambda = 1$. The greater microheterogeneity experienced by 4PBI under this condition is similar to the earlier experiments with C102, 2PBI, and $BP(OH)_2$. However, unusual excited states are not observed, unlike in those cases.

In the next step of the experiment, H_3O^+ ions in Nafion have been replaced by Na^+ or $(CH_3)_4N^+$ ions. Steady-state spectra of 4PBI are found to be different in these two kinds of membranes with different cations (Figures 1), unlike in our earlier experiments with C102 and 2PBI in which the spectral properties of the fluorescent probes remain the same in the two cation-exchanged membranes.[20] In Na^+-exchanged membranes, at $\lambda = 6$, the absorption spectrum exhibits two distinct maxima at 310 and 360 nm. These are characteristic absorption regions of cationic and tautomeric forms, C and T, respectively. In the $(CH_3)_4N^+$-exchanged membrane, however, the 350 nm band is prominent, with only a shoulder at 310 nm. This difference in the absorption spectra makes it possible to distinguish between the two kinds of cation-exchanged membranes using 4PBI. This is in contrast to earlier results with C102, 2PBI, and $BP(OH)_2$.[17,20,21] It may be noted here that the pK_a of C as well as T is 4.17 in neat aqueous solutions. From the absorption studies reported above, it is apparent that the values of pK_a are no longer the same in the microheterogeneous environments of $(CH_3)_4N^+$-exchanged and Na^+-exchanged Nafion membranes. It appears that in Na^+-exchanged membranes there is an increased propensity for the formation of C compared to that of T. The spectrum in $(CH_3)_4N^+$-exchanged membrane is closer to that in neat aqueous solutions at pH 3. This is in line with a model that we proposed earlier in which $(CH_3)_4N^+$ ions are localized more toward the negatively charged interface, thus offering a more bulk-water-like environment to an incorporated fluorescent molecule.[18] In Na^+-exchanged membranes, there is a more uniform distribution of Na^+ ions, so 4PBI molecules sample the interface in Na^+-exchanged membranes to a greater extent than in $(CH_3)_4N^+$-exchanged membranes and consequently, experience a greater extent of microheterogeneity.

T* fluorescence is overwhelmingly predominant in Na^+-exchanged membranes for $\lambda_{ex} > 350$ nm. Excitation at shorter wavelengths, however, gives rise to fluorescence from C* as well as T*. Excitation spectra depend on the wavelength at which the fluorescence is monitored. For $\lambda_{em} = 400$ nm, a very good overlap with the 310 nm absorption band is obtained, with a minor band at 360 nm. However, the excitation spectrum for $\lambda_{em} = 500$ nm exhibits a nearly perfect overlap with the 360 nm band. This indicates that the fluorescence at 400 nm is predominantly from C*, with a small contribution from T*, whereas that at 500 nm is exclusively from T*. Hence, the presence of the two ground-state isomers, C and T, is established. The absence of dication D marks the significantly lower acidity of the Na^+-exchanged membrane, in comparison to that of the native membrane. The characteristics of emission in $(CH_3)_4N^+$-exchanged membranes are different from those in Na^+-exchanged membranes. The fluorescence studies confirm the decreased propensity of formation of C in $(CH_3)_4N^+$-exchanged membranes. C* emission at 400 nm is not observed upon exciting 4PBI in $(CH_3)_4N^+$-exchanged membranes at 310 nm. However, the excitation spectrum does not have a perfect overlap with the absorption spectrum, unlike in the case of Na^+-exchanged membranes. This may be rationalized in light of the smaller fluorescence quantum yield of C* compared to that of T*.

Upon dehydration of the Na^+-exchanged membranes, there is no spectral shift in the absorption spectrum, but the 310 nm band becomes more prominent than the 360 nm band. This may indicate a shift in the ground-state equilibrium toward C. Unlike in the native membrane, the fluorescence spectrum now becomes strongly dependent on the wavelength of excitation, signifying a greater ground-state heterogeneity experienced by the fluorophore at a lower water content. The dehydration of

dx.doi.org/10.1021/jp303924a | J. Phys. Chem. B 2012, 116, 9992−9998

the Na^+-exchanged membrane results in a slight blue shift and a narrower fluorescence spectrum, indicating a more rigid environment. The fluorescence spectrum obtained upon 295 nm excitation for $\lambda = 6$ exhibits a prominent T* band and a shoulder for C* emission. At lower hydration levels of $\lambda = 1$, C* emission becomes more prominent. A decrease in the hydration level does not seem to affect the absorption and excitation spectra in $(CH_3)_4N^+$-exchanged Nafion. The fluorescence spectrum in $(CH_3)_4N^+$-exchanged membranes undergoes a marked blue shift upon decreasing the water content. This indicates a smaller ground-state inhomogeneity in the microenvironment. The blue shift in fluorescence may also be due to a more restricted environment resulting from the decreased availability of water. The invariance in the absorption spectrum upon drying is similar to that of native membranes. However, in native membranes there is no change in the shape of the fluorescence spectrum upon decreasing the water content. One of the reasons for a shift in the fluorescence spectrum is the change in polarity of the medium around the fluorophore. In native membranes, the fluorophore does not experience a significant change in polarity upon drying. However, in $(CH_3)_4N^+$-exchanged membranes, the $(CH_3)_4N^+$ ions form a layer adjacent to the sulfonate groups of Nafion. This layer repels the monocationic 4PBI molecules, which then sample the bulk-water-like region to a greater extent. Thus, in $(CH_3)_4N^+$-exchanged membranes at $\lambda = 6$, a large number of water molecules surround the fluorophore. At $\lambda = 1$, where the bulklike water is lost upon drying, 4PBI experiences a more apolar environment because of the methyl groups.

4PBI in the Na^+-exchanged membrane has been excited at 295 nm as well as at 340 nm for time-resolved fluorescence studies because these two wavelengths predominantly excite the C form and the T form, respectively. For $\lambda = 6$, the decays recorded at the blue end (λ_{em} = 375 and 420 nm) of the fluorescence spectrum are biexponential and depend strongly on the excitation wavelength. The decays at the red end of the fluorescence spectrum are single-exponential and superimposable for the two excitation wavelengths. Interestingly, the decays with λ_{ex} = 295 nm become markedly slower upon the drying of the membrane, but those with λ_{ex} = 340 nm change very little (Figure 3, Table 2). These observations indicate that 295 nm light predominantly excites the 4PBI molecules that are in a waterlike environment whereas 340 nm light excites those near the sulfonate groups. The lifetimes mark the microheterogeneity of the Na^+-exchanged membrane as well. The 1.2−1.5 ns component, observed at the blue end, is assigned to C* emission, and the longer component, which becomes the lone component at the red end, is assigned to T* emission. The increase in the T* lifetime with the emission wavelength is in line with the steady-state results and indicates that 4PBI molecules in the T form experience a gradually changing microenvironment, even near the sulfonate groups.

The temporal behavior in $(CH_3)_4N^+$-exchanged membranes is different from that of Na^+-exchanged membranes. The decays are distinctly slower at lower levels of hydration (Figure 4, Table 3). This behavior is contrary to what we have observed for C102, 2PBI, and $BP(OH)_2$. With the earlier probes, no changes in the fluorescence decays have been observed upon dehydration of the membrane. This has been explained on the basis of the invariance in their microenvironments upon drying the membrane.[20] We have proposed that the $(CH_3)_4N^+$ ions are arranged in the vicinity of the sulfonate groups, forming a uniform bilayer. It is well known that these ions themselves do

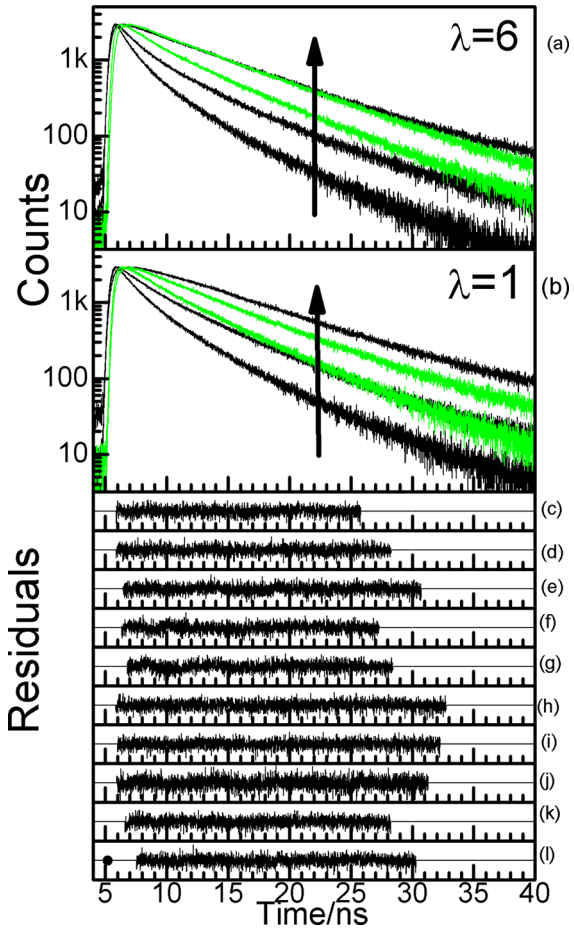

Figure 3. (a, b) Fluorescence decays of 4PBI in Na^+-exchanged membranes at (a) $\lambda = 6$ and (b) $\lambda = 1$. λ_{ex} = 295 nm (black) and 340 nm (green). (c−l) Weighted residuals for fits to the data in) and b. (c−e) $\lambda = 6$, λ_{ex} = 295 nm, λ_{em} = (c) 375, (d) 420, and (e) 510 nm. (f, g) $\lambda = 6$, λ_{ex} = 340 nm, λ_{em} = (f) 420 and (g) 510 nm. (h−j) $\lambda = 1$, λ_{ex}= 295 nm, λ_{em} = (h) 375, (i) 420, and (j) 510 nm. (k, l) $\lambda = 1$, λ_{ex} = 340 nm, λ_{em} = (k) 420 and (l) 510 nm.

not possess a hydration shell,[26] so the fluorescent probe experiences bulklike water only, not interfacial water. The 1.8 ns component observed at the blue end of the spectrum is ascribed to the T* in a more waterlike environment whereas the longer one is ascribed to the fluorophore in a less-polar environment. Upon decreasing the water content, the short component vanishes and only T* emission from a less-polar environment is observed. The fluorescence decays are slower at the red end of the spectrum than those recorded at the blue end, indicating that the fluorophore experiences a greater inhomogeneity in $(CH_4)_3N^+$-exchanged membranes. Cations displace a significant amount of water, thus the hydrogen-bonding structure might change. This may be a reason for the inhomogeneity experienced by the fluorophore. The long component of 6 ns slows down to 9 ns upon decreasing the water content in the membrane. This is concomitant with the increase in the fluorescence quantum yield. The reason is ascribed to a more rigid environment experienced by the probe upon drying.

So far, it is evident that there is a preferential formation of one form of the cationic form of 4PBI over the other in cation-exchanged membranes. In Na^+-exchanged membranes, both C and T forms are observed, whereas in $(CH_3)_4N^+$-exchanged

dx.doi.org/10.1021/jp303924a | J. Phys. Chem. B 2012, 116, 9992−9998

Table 2. Temporal Features of the Fluorescence of 4PBI in Na^+-Exchanged Nafion at Higher-Hydration ($\lambda = 6$) and Lower-Hydration ($\lambda = 1$) Levels

		$\lambda = 6$					$\lambda = 1$				
λ_{ex}/nm	λ_{em}/nm	τ_1/ns	τ_2/ns	a_1	a_2	χ^2	τ_1/ns	τ_2/ns	a_1	a_2	χ^2
	375	1.20	4.37	0.89	0.11	1.02	1.52	4.87	0.71	0.29	1.03
295	420	1.57	5.65	0.65	0.35	0.98	1.89	6.05	0.47	0.53	0.98
	510		7.30		1.00	1.06		7.65		1.00	1.77
340	420		5.57		1.00	1.08		5.28		1.00	1.05
	510		7.65		1.00	1.09		6.62		1.00	1.01

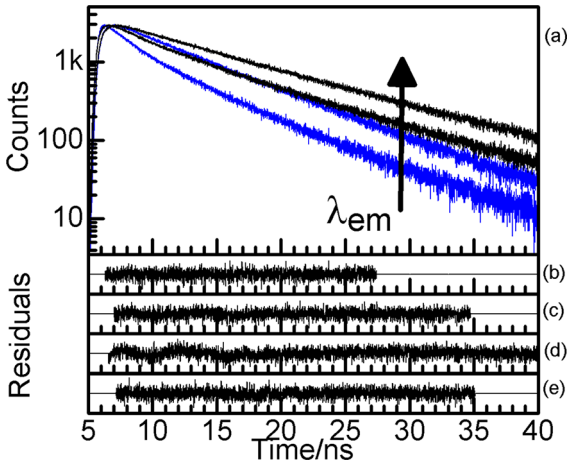

Figure 4. (a) Fluorescence decays of 4PBI in $(CH_3)_4N^+$-exchanged membranes at $\lambda = 6$ (blue) and $\lambda = 1$ (black). The faster decay at each λ value corresponds to $\lambda_{em} = 410$ nm, and the slower one corresponds to $\lambda_{em} = 540$ nm. (b–e) Weighted residuals for fits to the data in a. (b) $\lambda = 6$ and $\lambda_{em} = 410$ nm. (c) $\lambda = 6$ and $\lambda_{em} = 540$ nm. (d) $\lambda = 1$ and $\lambda_{em} = 410$ nm. (e) $\lambda = 1$ and $\lambda_{em} = 540$ nm.

membranes, there is a preference for T and T*. However, a shift in equilibrium toward C is observed in Na^+-exchanged membranes. This observation is in keeping with the existing knowledge that confined media such as micelles and membranes affect the dynamics of proton transfer significantly.[8,27–36] In this connection, one may recall the studies performed by Fayer and co-workers on the slower water orientation dynamics of water molecules in Nafion membranes.[27] These experiments have established that there is more than one kind of water species present inside the water channels of a Nafion membrane.[28] Proton-transfer processes take place in various ways inside membranes because there are different types of water present in them. Water in confined systems may either exhibit features that are characteristic of bulk water where proton conductivity involves charge transfer only or show a high orientation effect because of the small availability of water molecules.[35] Another experiment has shown that the water around hydrophobic molecules exhibits slower dynamics than that farther away from them. Thus, it can be said that various types of nanoenvironments exist within the water channels of Nafion and the ions present also influence the nature of the water in these channels. Na^+ ions possess a hydration shell containing water that is different from the bulk. $(CH_3)_4N^+$ ions, however, do not possess a hydration shell, but the apolar methyl groups can slow down the dynamics of water around them. This difference in environments in different cation-exchanged membranes affects the water dynamics. This may arise from the interactions of water molecules with the sulfonate groups or polymer or the cations present inside the membrane. Consequently, the slower dynamics of water molecules leads to slower proton-transfer dynamics. Furthermore, the range of environments that exists inside the nanochannels of Nafion may be attributed to the preferential stabilization of one isomer over another in different cation-exchanged membranes.

CONCLUSIONS

The monocationic, T, form of 2-(4′-pyridyl)benzimidazole is found to coexist with its dicationic, D, form in native Nafion, with no signature of the other monocation, C. Thus, Nafion is found to provide a microheterogeneous environment that selectively promotes one of the two possible monocationic species in this fluorophore. The importance of electrostatic interactions in partially dehydrated membranes is manifested in the lifetimes of the T* form, indicating the predominance of the T* molecules near the negatively charged walls of the water channels. Upon cation exchange by Na^+ ions, the preference for the C form is increased over that for the T form. The situation is reversed in $(CH_3)_4N^+$-exchanged membranes. Interestingly, 4PBI is found to be an efficient probe in differentiating between the two cation-exchanged membranes at lower hydration levels as well, unlike the fluorescent probes used earlier. The experiments performed in this article further support the prevailing contention of different types of water molecules present inside the nanochannels of Nafion. The environment of water is affected by the nature of the ions, as manifested in the spectral behavior of fluorescent probe 4PBI. This article supports the contention that different cations distribute themselves differently inside the water channels. Thus, the 4PBI probe is able to mark the microhetrogeneity in cation-exchanged Nafion membranes more efficiently than earlier probes. The complex microenvironment in the nanochannels of Nafion has been better understood using this probe.

Table 3. Temporal Features of the Fluorescence of 4PBI in $(CH_3)_4N^+$ Nafion at Higher-Hydration ($\lambda = 6$) and Lower-Hydration ($\lambda = 1$) Levels

	$\lambda = 6$					$\lambda = 1$				
λ_{em}/nm	τ_1/ns	τ_2/ns	a_1	a_2	χ^2	τ_1/ns	τ_2/ns	a_1	a_2	χ^2
410	1.84	5.95	0.60	0.40	1.03		7.81		1.00	1.12
540		6.65		1.00	1.01		9.24		1.00	1.04

dx.doi.org/10.1021/jp303924a | J. Phys. Chem. B 2012, 116, 9992–9998

AUTHOR INFORMATION

Corresponding Author

*E-mail: anindya@chem.iitb.ac.in. Phone: +91-22-2576-7149. Fax: +91-22-2576-3480.

Notes

The authors declare no competing financial interest.

ACKNOWLEDGMENTS

We thank the Naval Research Board, India for generous research grants. E.S.S.I. thanks CSIR, India for a senior research fellowship. We thank Mr. Vijaykant Khorwal for his help with the purification and crystallization of 4PBI. We thank one of the reviewers for insightful comments.

REFERENCES

(1) Mauritz, K. A.; Moore, R. B. *Chem. Rev.* **2004**, *104*, 4535−4585.
(2) Gelbard, G. *Ind. Eng. Chem. Res.* **2005**, *44*, 8468−8498.
(3) Kreuer, K,-D.; Paddinson, S. J.; Spohr, E; Schuster, M. *Chem. Rev.* **2004**, *104*, 4367−4416.
(4) Serpico, J. M.; Ehrenberg, S. G.; Fontanella, J. J.; Jiao, X.; Perahia, D.; McGrady, K. A.; Sanders, E. H.; Kellogg, G. E.; Wnek, G. E. *Macromolecules* **2002**, *35*, 5916−5921.
(5) Starkweather, H. W., Jr. *Macromolecules* **1982**, *15*, 320−323.
(6) Anantaraman, A. V.; Gardner, C. L. *J. Electroanal. Chem.* **1996**, *414*, 115−122.
(7) Schmidt-Rohr, K; Chen, Q *Nat. Mater.* **2008**, *7*, 75−83.
(8) Moilanen, D. E.; Piletic, I. R.; Fayer, M. D. *J. Phys. Chem. C* **2007**, *111*, 8884−8891.
(9) Gebel, G. *Polymer* **2000**, *41*, 5829−5838.
(10) Gierke, T. D.; Munn, G. E.; Wilson, F. C. *J. Polym. Sci., Polym. Phys. Ed.* **1981**, *19*, 1687−1704.
(11) Rollet, A.-L.; Diat, O.; Gebel. *J. Phys. Chem. B* **2002**, *21*, 3033−3036.
(12) Rubatat, L.; Rollet, A.-L.; Gebel, G.; Diat, O. *Macromolecules* **2002**, *35*, 4050−4055.
(13) Rubatat, L.; Gebel, G.; Diat, O. *Macromolecules* **2004**, *37*, 7772−7783.
(14) Haubold, H.-G.; Vad, T.; Jungbluth, H.; Hiller, P. *Electrochim. Acta* **2001**, *46*, 1559−1563.
(15) Kreuer, K. D. *J. Membr. Sci.* **2001**, *185*, 29−39.
(16) Kim, M -H.; Glinka, C. J.; Grot, S. A.; Grot, W. G. *Macromolecules* **2006**, *39*, 4775−4787.
(17) Iyer, E. S. S.; Datta, A. *J. Phys. Chem. B* **2012**, *116*, 5302−5307.
(18) Burai, T. N.; Datta, A. *J. Phys. Chem. B.* **2009**, *113*, 15901−15906.
(19) Mukherjee, T. K.; Datta, A. *J. Phys. Chem. B* **2006**, *110*, 2611−2617.
(20) Iyer, E. S. S.; Datta, A. *J. Phys. Chem. B* **2011**, *115*, 8707−8712.
(21) Iyer, E. S. S.; Samanta, D.; Dey, A.; Kundu, A; Datta., A. *J. Phys. Chem. B* **2012**, *116*, 1586−1592.
(22) Novo, M.; Mosquera, M.; Rodriguez-Prieto, F. *J. Phys. Chem.* **1995**, *99*, 14726−14732.
(23) Novo, M.; Mosquera, M.; Rodriguez-Prieto, F. *Can. J. Chem.* **1992**, *70*, 823−827.
(24) Brown, R. O.; Eniwlstle, N.; Hepworth, J. D.; Hodgson, K. W.; May, B. *J. Phys. Chem.* **1982**, *86*, 2418−2420.
(25) Slade, S.; Campbell, S. A.; Ralph, T. R.; Walsch, F. C. *J. Electrochem. Soc. A* **2002**, *49*, 1556−1564.
(26) Marcus, Y. *Ion Properties*; Marcel Dekker: New York, 1997.
(27) Piletic, I. R.; Moilanen, D. E.; Levinger, N. E.; Fayer, M. D. *J. Phys. Chem. A* **2006**, *110*, 4985−4999.
(28) Spry, D. B.; Glusac, G. K.; Moilanen., D. E.; Fayer, M. D. *J. Am. Chem. Soc.* **2007**, *129*, 8122−8130.
(29) Spry, D. B.; Glusac, G. K.; Moilanen, D. E.; Fayer, M. D. *J. Am. Chem. Soc.* **2004**, *129*, 4535.
(30) Spry, D. B .; Fayer, M. D. *J. Phys. Chem. B* **2009**, *113*, 10210.
(31) Moilanen, D. E.; Spry, D. B.; Fayer, M. D. *Langmuir* **2008**, *24*, 3690.
(32) Piletic, I. R.; Moilanen, D. E.; Levinger, N. E.; Fayer, M. D. *J. Am. Chem. Soc.* **2006**, *128*, 10366.
(33) Tielrooij, K. J.; Timmer, R. L. A.; Bakker, H. J.; Bonn, M. *Phys. Rev. Lett.* **2009**, *102*, 1983031−1983036.
(34) Bakulin, A. A.; Pshenichnikov, S. M.; Bakker, H. J.; Petersen, C *J. Phys. Chem. A* **2011**, *115*, 1821−1829.
(35) Tielrooij, K. J.; Paparo, D.; Piatkowsky, L.; Bakker, H. J.; Bonn, M. *Biophys. J.* **2009**, *97*, 2484−2492.
(36) Siwick, B. J.; Bakker, H. J. *J. Am. Chem. Soc.* **2007**, *129*, 13412−13420.